

See discussions, stats, and author profiles for this publication at: <https://www.researchgate.net/publication/231393447>

# Effect of the Alkali Metal Activator on the Properties of Fly Ash-Based Geopolymers

ARTICLE *in* INDUSTRIAL & ENGINEERING CHEMISTRY RESEARCH · SEPTEMBER 1999

Impact Factor: 2.59 · DOI: 10.1021/ie980804b

---

CITATIONS

156

---

READS

176

2 AUTHORS, INCLUDING:



Jannie S J Van Deventer

University of Melbourne

312 PUBLICATIONS 10,060 CITATIONS

SEE PROFILE

# Effect of the Alkali Metal Activator on the Properties of Fly Ash-Based Geopolymers

J. G. S. van Jaarsveld and J. S. J. van Deventer\*

Department of Chemical Engineering, The University of Melbourne, Parkville, Victoria 3052, Australia

The alkali and alkali earth metal cations present during the formation of most known aluminosilicate structures have a very significant effect on both the physical and chemical properties of the final product. Geopolymers are no exception, although this effect has not been thoroughly quantified and in the case of waste-based geopolymers it has not received any significant attention. The present study investigates the effect of mainly  $\text{Na}^+$  and  $\text{K}^+$  on the physical and chemical properties of fly ash-based geopolymeric binders both before and after setting has occurred. A variety of tests were conducted, including rheological measurements, various leaching tests, compressive strength testing, specific surface area determinations, and infrared spectroscopy (IR). It is concluded that the alkali metal cation controls and affects almost all stages of geopolymerization, from the ordering of ions and soluble species during the dissolution process to playing a structure-directing role during gel hardening and eventual crystal formation.

## Introduction

The importance and effect of the type of alkali metal ion present during the synthesis of aluminosilicate structures have been acknowledged by numerous authors,<sup>1–4</sup> and in the case of some zeolitic structures it has been studied extensively.<sup>5,6</sup> As far as geopolymerization is concerned, the role played by alkali and alkali earth metals has been acknowledged as having certain structural implications<sup>7–9</sup> but it has never been properly studied, except for contributions by Davidovits<sup>10,11</sup> that belong to the patent literature and deal exclusively with metakaolinite-based systems. This discussion will start to address this issue by investigating the geopolymerization of fly ash as described in previous publications.<sup>7,8</sup> The complexity of studying nonideal systems such as the present arises from the fact that fly ash is used in the synthesis of the various geopolymeric matrixes, and although this provides for data that can be applied easily in practice, the presence of small amounts of impurities and heavy metals can be expected to have an unknown effect on all experimental results. Since very little experimental evidence exists in the literature, the contribution of the present study to the knowledge base of waste-based geopolymer synthesis is novel to a large extent. It should finally be mentioned that the discussion would be confined to the most widely used alkali metal cations i.e.,  $\text{K}^+$  and  $\text{Na}^+$ .

## Background and Literature

Certain physical properties of geopolymers discussed by Davidovits<sup>9</sup> appeared to be affected by the type of alkali metal present during synthesis. Most other studies<sup>12,13</sup> concerning geopolymerization or applications thereof did not specifically investigate this effect. It was mentioned previously<sup>14</sup> that the type of metal cation affects most of the physical and chemical properties of the final product and as such plays an important role

during synthesis and also in determining the long-term durability of geopolymeric binders.

In the present study, where fly ash and kaolinite provide the bulk of the geopolymeric binder, the mechanism will include an initial dissolution step where the alkali solution not only hydrolyzes the surface of mineral particles but also dissolves a small amount of Al and Si species. These dissolved species will react with already dissolved silicate ions and polycondense to form a gel that is transformed to the final structure either through another dissolution and crystallization process<sup>2,15</sup> or through a solid-state mechanism as proposed by Wang and Scrivener<sup>16</sup> for alkali activated slag cements. The effect of alkali metal cations on any of the above processes can therefore be expected to also affect the final structure and properties. The initial dissolution process is caused by the presence of  $\text{OH}^-$  ions and is thought to be independent of the type or concentration of cation present<sup>15</sup> although this fact has not been thoroughly investigated. Kostinko<sup>17</sup> concluded that, besides temperature, the relative importance of the different compositional ratios to the reaction time of zeolite synthesis is the following:  $\text{H}_2\text{O}/\text{Na}_2\text{O} > \text{Na}_2\text{O}/\text{SiO}_2 > \text{SiO}_2/\text{Al}_2\text{O}_3$ . Since the formation of amorphous zeolites with low porosity depends on a low water content in the synthesis mixture, the first ratio will also have structural implications with respect to the final product. It is a well-known fact that alkali and alkali earth metal cations also play a charge balancing role where Al substitutes for Si in the aluminosilicate structure and the presence of these cations will therefore affect the  $\text{SiO}_2/\text{Al}_2\text{O}_3$  ratio of the final structure.

It is during the final polycondensation or crystallization process that these cations are thought to play a major role in determining the final structure and therefore its physical and chemical properties. The formation of different zeolites in the presence of different alkali metal cations is very well documented,<sup>1,2</sup> and Davidovits also mentions geopolymers, where the only difference in chemical composition is the type of metal cation present.<sup>9</sup> The structure-directing role played by

\* To whom correspondence should be addressed. E-mail: jsj.van\_deventer@chemeng.unimelb.edu.au.

**Table 1. Composition of Fly Ash as Determined by Fusion and XRF Analysis (Mass %)**

element as oxide	SASOL	Tarong	Port Augusta	Port Hedland	Macquarie
SiO <sub>2</sub>	50.1	61.4	48.5	49.7	59.9
Al <sub>2</sub> O <sub>3</sub>	28.3	33.0	29.6	24.6	21.6
CaO	8.2	0.6	6.1	4.9	2.9
Fe <sub>2</sub> O <sub>3</sub>	4.0	1.1	4.6	12.7	4.7
MgO	2.0	0.3	2.3	1.4	1.4
TiO <sub>2</sub>	1.5	2.0	2.5	1.5	0.8
Na <sub>2</sub> O	0.5	0.1	3.7	0.0	0.4
K <sub>2</sub> O	0.9	0.1	0.9	0.5	2.3
SO <sub>3</sub>	0.4	0.0	0.3	0.4	0.2
loss on ignition	4.1	1.4	1.5	4.3	5.8

these cations during synthesis arises from the fact that they are very energetically hydrated and the center of minute water clusters in solution.<sup>5</sup> These water molecules can be partly replaced by silicate or aluminosilicate species resulting in the formation of precursors to the nuclei that would serve as points of further structural development. McCormick and Bell<sup>4</sup> also observed that small alkali metal cations produce the highest rates of zeolite nucleation. In this capacity the cations serve as templates and have a structure-directing role. Polymerization may finally also occur by chemical bonding to surface OH groups on existing undissolved waste particles, and the cation is expected to play a similar role as discussed previously. It should be kept in mind, however, that the addition of dissolved species to an existing structure depends on a proper fit between the unit that is being added and the underlying structure.

When hydration of metal cations is considered, it must be kept in mind that the sizes of K<sup>+</sup> (1.33 Å) and Na<sup>+</sup> (0.97 Å) ions are substantially different, leading to a lower surface charge density in the case of K. The size difference between K and Na will therefore not only impact on structure formation from a physical point of view but also from a chemical and hydration point of view, as a K ion is expected to be associated with more water molecules than the comparable Na ion if all other factors remain constant. This effect could contribute to the conclusion drawn by McCormick and Bell<sup>4</sup> that larger cations seem to increase the extent of condensation during the formation of aluminosilicate structures.

## Experimental Section

**Materials.** Fly ash used in the synthesis of matrixes F1, F2, G1, and G2 was obtained from SASOL at Sasolburg, South Africa, the fly ash used in matrixes H1–H4 and S4–S38 was from Tarong power station in Queensland, Australia, and that used in matrixes B26–B37 from Lake Macquarie, New South Wales, Australia. Other fly ash discussed originated from Port Augusta, South Australia, and Port Hedland, Western Australia. All fly ashes were of coal origin, with particle sizes in the order of 50% smaller than 25 µm and chemical compositions as shown in Table 1. Kaolinite, grade HR1, was obtained from Commercial Minerals, Sydney, Australia. Silicate solutions were supplied by PQ Australia, Sydney, under the brand names of KASIL 2236 (11 wt % K<sub>2</sub>O, 24.6 wt % SiO<sub>2</sub>) and Vitrosol N40 (8.9 wt % Na<sub>2</sub>O and 28.7 wt % SiO<sub>2</sub>). All experiments were performed using the same batches of reagents and starting materials. Distilled water was used throughout.

**Synthesis.** Sample preparation was performed as described previously<sup>8</sup> with at least a 7-day waiting period being observed before any tests were performed.

Samples were prepared by mixing of the dry reagents for a period of 10 min, followed by the addition of the liquid component and further mixing for 15 min. In each case the samples were cast in 50 mm cubes, vibrated for 5 min, and allowed to set at 30 °C for 24 h before being removed from the moulds and kept at room temperature for another 6 days. In the case of matrixes F, G, and H heavy metal cations were added to the reaction mixture during mixing as a solution of Cu(NO<sub>3</sub>)<sub>2</sub> or Pb(NO<sub>3</sub>)<sub>2</sub> in water. Tables 2 and 3 summarize the compositions of these matrixes. Tables 4 and 5 contain the compositions of matrixes that do not contain added metal contaminants and will be used mainly for assessing the effect of KOH, NaOH, Na silicate, and K silicate on structural properties such as specific surface area and compressive strength. It could well be noted that the amount of NaOH and KOH used in producing matrixes F1, F2, G1, and G2 was chosen such as to provide for equal total molar amounts of Na and K in the structures of all the matrixes in Table 2.

Where M<sub>2</sub>O/SiO<sub>2</sub> ratios are quoted (M = K and/or Na), these represent the soluble component of the mix before geopolymerization has taken place and do not take into account any subsequent dissolution from either the kaolinite or fly ash. This last component is very difficult to quantify as different fly ashes and kaolinite from different sources exhibit varying degrees of surface reactivity. An attempt was made to qualitatively discuss this effect by utilizing a simple leaching test, discussed later in this section. From the values obtained it was not only evident that surface leaching contributes very little to the total concentration of Al and Si but also that kaolinite and fly ash leach Al and Si at different rates. Initial mix designs did not take this into account, and various amounts of kaolinite were therefore added to mixes on the basis of final workability rather than chemical reactivity.

**Yield Strength Measurements.** To investigate the effect of various factors on the setting characteristics of the geopolymer paste, the early yield strengths of various mixes were measured by a vane rheometer as described by De Kretser.<sup>18</sup> A fresh mixture was made for every measurement, and all experiments were repeated three times. Care was taken to minimize disturbance of the gel structure before any measurements were made.

**Acid Resistance.** Acid resistance tests were conducted on matrixes B26–B37 by immersing the 50 mm cubes in a solution of 1 M hydrochloric acid at a solid/liquid ratio of 1:4. The mass loss and final pH were measured after 34 days, the latter being less than 1.0 in each case.

**Compressive Strength Testing.** Compressive strength testing was performed as per AS 1012.9<sup>19</sup> using 50 mm diameter cylinders with a 1:2 diameter-to-length ratio. Three cylinders of each sample were tested, averaging the experimental values obtained. All samples were tested after 14 days. An Amsler FM 2750 compressive strength testing apparatus was used.

**Leaching Tests.** Samples submitted to environmental leaching tests were crushed and sieved into particle size fractions, the latter being leached until equilibrium conditions were obtained. Leaching of each particle size fraction was conducted using a modified TCLP<sup>8,20</sup> procedure utilizing acetic acid buffered at pH = 3.3 by analytical grade sodium acetate. The solid/liquid ratio was kept at 1:25 and the temperature controlled at 30

**Table 2. Compositions of Matrixes Prepared from SASOL Fly Ash**

matrix	alkali metal	contaminant (mass %)	(K <sub>2</sub> O + Na <sub>2</sub> O)/SiO <sub>2</sub> (mol)	clay (mass %)	water/fly ash (mass ratio)	Al <sub>2</sub> O <sub>3</sub> /SiO <sub>2</sub> (mass ratio)
F1	Na	Cu (0.1)	1.14	15.0	0.2	0.57
F2	Na	Pb (0.1)	1.14	15.0	0.2	0.57
G1	K	Cu (0.1)	1.14	15.0	0.2	0.57
G2	K	Pb (0.1)	1.14	15.0	0.2	0.57

**Table 3. Compositions of Matrixes Prepared from Tarong Fly Ash with Added Metal Contaminants**

matrix	alkali metal	contaminant (mass %)	(K <sub>2</sub> O + Na <sub>2</sub> O)/SiO <sub>2</sub> (mol)	clay (mass %)	water/fly ash (mass ratio)	Al <sub>2</sub> O <sub>3</sub> /SiO <sub>2</sub> (mass ratio)
H1	K	Cu (0.1)	1.14	14.0	0.43	0.52
H2	K	Pb (0.1)	1.14	14.0	0.43	0.50
H3	Na	Pb (0.2)	0.94	14.0	0.45	0.46
H4	Na	Cu (0.2)	0.94	14.0	0.45	0.46

**Table 4. Compositions of Matrixes Prepared from Tarong Fly Ash Using Either KOH or NaOH**

matrix	hydroxide	silicate	(K <sub>2</sub> O + Na <sub>2</sub> O)/SiO <sub>2</sub> (mol)	clay (mass %)	water/fly ash (mass ratio)
S4	K	Na	0.58	31	1.12
S5	Na	Na	0.58	31	1.12
S6	K	Na	1.20	14	0.35
S7	Na	Na	1.04	14	0.36
S8	K	Na	1.05	21	0.43
S9	Na	Na	1.04	21	0.43
S11	K	Na	1.05	7	0.33
S12	Na	Na	1.02	7	0.33
S23	K	Na	1.94	7	0.34

°C. Equilibrium tests on matrixes were conducted by the use of stirred vessels with overhead impellers. This technique allowed for equilibrium to be attained in around 24 h with sampling being performed periodically over a 24-h period. Sampling was conducted by syringe, and the total sampling volume never exceeded 10% of the fluid volume, thus creating an average error of 5%. In a separate set of experiments the matrixes of Table 2 were also submitted to leaching by hydrochloric acid at pH = 3.3 with external pH control.

Apart from environmental leaching tests a comparative test was performed on certain fly ashes in order to compare the solubility of their Si- and Al-containing phases in both sodium and potassium hydroxide. These tests consisted of mixing the fly ash with a 1 M solution of either NaOH or KOH at 80 °C for 1 h. The solid/liquid ratio was 1:2. After this period samples were filtered and analyzed for Si and Al. Concentrations of all metals were determined using a Perkin-Elmer Optima 3000 ICP-OES, with scandium and/or cadmium as internal standard.

**Specific Surface Area, Infrared Analysis and X-ray Diffraction.** BET surface areas were determined for all samples by using a Micromeritics Flowsorb ASAP 2020 with a 30/70 ratio of N<sub>2</sub> and He, degassing for 18 h at 95 °C. Infrared spectra were recorded on a Mattson Galaxy 2020 spectrometer using the KBr pellet technique (0.5 mg powder sample mixed with 250 mg of KBr). X-ray powder diffraction data were obtained using a Phillips PW 1800 diffractometer with Cu K $\alpha$  radiation.

**Transmission Electron Microscopy.** Selected samples were submitted to study by transmission electron microscopy (TEM) on a JEOL CX 100 TEM fitted with an X-ray microanalysis system. The specimens were prepared by mechanically grinding the powder in ethanol, followed by ultrasonic agitation and precipitation on an amorphous carbon film. Electron diffraction data were obtained by manually measuring diffraction circle radii and calculating *d* spacing values

from the latter data, taking into account the other microscope parameters.

## Results and Discussion

**Dissolution and Early Setting Properties.** During the course of our earlier work it became obvious that the presence of either KOH or NaOH in synthesis mixtures had a fairly large effect on the rheology, mixing, and setting properties of geopolymer pastes. With the introduction of fly ash from different sources, this effect could not be ascribed to the presence of either Na or K in a predictable manner. This effect can be verified in Table 6, where the increase in yield stress between the 5-min and 10-min measurements differs quite substantially for the various fly ashes if all other variables remain constant. In each case the setting of mixtures containing fly ash from Port Augusta and Macquarie seems to be accelerated by the presence of Na and absence of K, whereas the opposite seems to be true for pastes containing fly ash from Tarong and Port Hedland. It should be kept in mind that the particles size distributions of these fly ashes are fairly similar although their mineralogy differs quite substantially. A detailed discussion of the mineralogy falls outside the scope of this investigation.

To quantify the relative amounts of Al and Si released by the fly ashes in an alkaline environment, leaching tests were conducted on the various fly ashes as described above. Table 7 summarizes these results, and it is of interest to note that in each case the dissolution of both Al and Si seems to be very dependent on the type of alkali metal cation present in the hydroxide solution. As the pH was the same in each case, the only difference between a fly ash leached with KOH and the same fly ash leached with NaOH was the type of cation present. As the cation appears to affect the amount of Al and Si being released, one would expect a subsequent effect on the structure that forms in the immediate vicinity of the fly ash particle as the Al/Si ratio of the aluminosilicate would differ depending on the alkali metal cation used. As was mentioned earlier, pastes containing the fly ash from Tarong and Port Hedland appeared to set faster in the presence of KOH compared to NaOH. These two fly ashes also appeared to leach more Al when contacted with KOH, and the Al/Si ratio in their respective leaching solutions was much higher than the same ratio when they were leached with NaOH. The fly ash from Port Augusta and Macquarie, however, contains an amount of K<sub>2</sub>O (Table 1) but presented fairly similar ratios of Al/Si during both leaching with NaOH and KOH. With reference to the



**Table 5. Compositions of Matrixes Prepared from Tarong Fly Ash Using Combinations of KOH and NaOH**

matrix	hydroxide	silicate	K <sub>2</sub> O/SiO <sub>2</sub> (mol)	Na <sub>2</sub> O/SiO <sub>2</sub> (mol)	(K <sub>2</sub> O+Na <sub>2</sub> O)/SiO <sub>2</sub> (mol)	clay (mass %)	water/fly ash (mass ratio)
S29	K, Na	Na	0.49	0.84	1.33	40	0.78
S31	K, Na	Na	0.16	1.30	1.46	40	0.78
S32	K, Na	Na	0.32	1.08	1.40	40	0.78
S33	K, Na	Na	0.71	0.66	1.37	40	0.75
S34	K, Na	Na	0.89	0.41	1.30	40	0.75
S36	K	K	1.61	0	1.61	7	0.29
S37	Na	K	0.60	1.21	1.81	7	0.31

**Table 6. Effect of NaOH and KOH on the Initial Yield Strengths for Pastes Containing Various Fly Ashes**

fly ash	H <sub>2</sub> O/SiO <sub>2</sub> (mol)	(K <sub>2</sub> O+Na <sub>2</sub> O)/SiO <sub>2</sub> (mol)	K <sub>2</sub> O/SiO <sub>2</sub> (mol)	Na <sub>2</sub> O/SiO <sub>2</sub> (mol)	yield stress (Pa)		% change 5 to 10 min
					5 min	10 min	
Port Augusta	19	0.28	0.09	0.19	275	300	9
Port Augusta	19	0.28	0.00	0.28	320	366	14
Port Augusta	31	0.28	0.09	0.19	17	20	18
Port Augusta	31	0.28	0.00	0.28	17	25	47
Port Hedland	19	0.28	0.09	0.19	357	2002	460
Port Hedland	19	0.28	0.00	0.28	885	1682	90
Macquarie	31	0.28	0.09	0.19	69	110	59
Macquarie	31	0.28	0.00	0.28	64	154	141
Tarong	31	0.28	0.09	0.19	116	136	17
Tarong	31	0.28	0.00	0.28	106	108	2

**Table 7. Al and Si Leached from Selected Fly Ashes by KOH and NaOH, Calculated as Mass % of Total Amount Present According to XRF Analyses<sup>a</sup>**

fly ash	NaOH			KOH		
	Al (%)	Si (%)	Al/Si	Al (%)	Si (%)	Al/Si
Macquarie	0.52	0.43	0.5	0.43	0.29	0.5
Port Hedland	1.25	0.41	1.7	0.92	0.17	3.3
Tarong	0.95	0.42	1.6	0.83	0.22	2.5
Port Augusta	0.79	0.32	1.7	0.60	0.26	1.6

<sup>a</sup> Ratios given are the relative ratio of actual concentration measured in solution (ppm/ppm).

**Table 8. Effect of Changing the Na<sub>2</sub>O/SiO<sub>2</sub> Ratio on Initial Setting Properties (Port Augusta)**

Na <sub>2</sub> O/SiO <sub>2</sub> (mol)	H <sub>2</sub> O/SiO <sub>2</sub> (mol)	yield stress (Pa)		% change 5 to 20 min
		5 min	20 min	
0.5	19	1260	2200	75
0.8	19	2200	3140	43
1.4	19	153	460	201
2.6	19	42	75	79
4.9	19	8390	30500	264

yield stress tests (Table 6), pastes containing these two fly ashes seemed to be accelerated by Na rather than K.

During synthesis the bulk solution contains a substantial amount of soluble silicate, and therefore, the dissolution of Al in the immediate vicinity of waste particles is not expected to alter structure formation in the bulk geopolymer phase. Phases forming in the immediate vicinity of fly ash particles, however, will be greatly affected by the presence of either K or Na as this will determine the Al/Si ratio and properties of the subsequent aluminosilicate structure such as compressive and bonding strengths.

Tables 8 and 9 provide some interesting information into the gel-formation characteristics of the reaction. It is apparent that for both KOH and NaOH an increase in the ratio M<sub>2</sub>O/SiO<sub>2</sub> (where M is Na or K) will decrease the viscosity of the mixture at a given time compared to a mixture with a lower such ratio. For any mixture with a fixed M<sub>2</sub>O/SiO<sub>2</sub> ratio, however, setting will proceed but usually at a slower speed than for lower M<sub>2</sub>O/SiO<sub>2</sub> ratios. At very high M<sub>2</sub>O/SiO<sub>2</sub> ratios the increase in viscosity is partly caused by the amount of

**Table 9. Effect of Changing the K<sub>2</sub>O/SiO<sub>2</sub> Ratio on Initial Setting Properties (Port Augusta)**

K <sub>2</sub> O/SiO <sub>2</sub> (mol)	H <sub>2</sub> O/SiO <sub>2</sub> (mol)	yield stress (Pa)		% change 5 to 20 min
		5 min	20min	
0.2	19	1260	5750	356
0.4	19	358	1520	325
0.9	19	200	248	24
1.7	19	35	88	150
3.4	19	2	7	250
5.1	19	7200	30400	322

solids added in the form of MOH in order to increase the alkalinity to this level. In the case of both Na (Table 8) and K (Table 9) there seems to be a decrease followed by an increase in the speed of setting as well as the absolute value of the yield stress as the M<sub>2</sub>O/SiO<sub>2</sub> ratio is increased. This effect is most probably caused by a number of factors: (a) An increased alkalinity better stabilizes and advances the dissolution of both Si and Al species.<sup>1,2</sup> (b) An increased M<sub>2</sub>O/SiO<sub>2</sub> ratio will increase nucleation and crystal growth,<sup>6</sup> and this effect will provide for the expulsion of water from the newly formed structure,<sup>7</sup> leading to an initial decrease in viscosity. (c) The overall decrease in the ratio H<sub>2</sub>O/M<sub>2</sub>O will serve to also increase nucleation and crystal growth as reported by Hu and Lee.<sup>6</sup> One would expect however that there will be certain physical constraints as to the maximum values of these ratios and the high yield stresses observed for both high and low M<sub>2</sub>O/SiO<sub>2</sub> ratios are results of these effects. At low M<sub>2</sub>O/SiO<sub>2</sub> ratios not enough OH<sup>-</sup> ions are present to adequately stabilize the solution and polymerization proceeds fairly quickly leading to high viscosity values with dissolution rates also expected to be lower.

Finally the presence of certain preferred stoichiometric reaction ratios<sup>3</sup> could also affect the stability of the gel phase leading to a quite stable paste around K<sub>2</sub>O/SiO<sub>2</sub> = 0.9 (Table 9) and Na<sub>2</sub>O/SiO<sub>2</sub> = 0.8 (Table 8). This point is not necessarily that of greatest viscosity but rather equilibrium where the rates of structure formation and breakdown are closest to equal. The points of lowest absolute viscosity represent a high release rate of water that momentarily keeps the viscosity down with the high alkali content creating a fairly stable environment for dissolution and polymerization. At M<sub>2</sub>O/SiO<sub>2</sub>

**Table 10. Effect of Other Ions on the Early Yield Stress of Geopolymeric Pastes (Port Augusta)**

compd	amt added (mol of metal cation)	H <sub>2</sub> O/SiO <sub>2</sub> (mol)	Na <sub>2</sub> O/SiO <sub>2</sub> (mol)	10 min yield stress (Pa)
NaOH		31	0.28	25
CaO	0.007	31	0.33	250
CaCO <sub>3</sub>	0.007	31	0.33	233
CaCl <sub>2</sub>	0.007	31	0.33	944
MgO	0.007	31	0.33	183
NaCl	0.01	31	0.41	350
Na <sub>2</sub> SO <sub>4</sub>	0.01	31	0.41	99

**Table 11. Compressive Strengths (MPa) and Specific Surface Area Values (m<sup>2</sup>/g) for Matrixes Containing Metal Contaminants Measured after 14 Days**

matrix	contaminant	alkali metal	compressive strength	specific surface area
F1	Cu (0.1%)	Na	43.8	8.8
G1	Cu (0.1%)	K	51.4	16.4
H1	Cu (0.1%)	K	4.5	9.3
H2	Pb (0.1%)	K	7.3	12.2
H3	Pb (0.2%)	Na	18.1	7.8
H4	Cu (0.2%)	Na	16.5	4.3

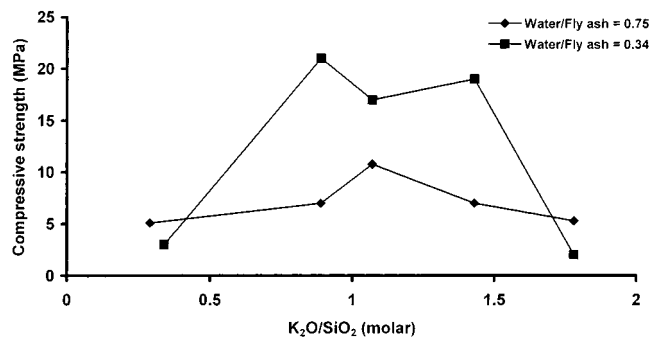
ratios higher than these the increased solid content of the paste starts to become a destabilizing factor while most added Na or K ions cannot be accommodated in the final structure.

Table 10 presents a comparison of changes in the 10-min yield stress measurements of pastes containing small amounts of Ca and Mg. These are compared with that obtained for a similar paste containing only NaOH at approximately the same Na<sub>2</sub>O/SiO<sub>2</sub> ratio. From the results it is obvious that the presence of both Ca and Mg increases the 10-min yield strength. This is mainly due to the formation of gellike Ca and Mg silicates and does not reflect the final setting properties of the geopolymer mixes. Practical experience showed that these gel structures containing Ca and Mg are very stable and in most cases final setting is delayed substantially. With reference to Tables 1 and 6, the natural Ca content of the various fly ashes does not seem to affect their reactivity accordingly and one could conclude that the Ca in these fly ashes is probably less available for dissolution. From Table 10 the effect of anions can also be seen very clearly, especially in the case of the Cl ion, which increased the yield stress in both the cases of NaCl and CaCl<sub>2</sub>. Ca seems to have a greater effect than Mg while the addition of CaCO<sub>3</sub> does not seem to have a substantially different effect from adding CaO. The accelerating effect caused by CaCl<sub>2</sub> has been attributed<sup>21,22</sup> to various mechanisms, including catalytic effects toward the polymerization of silica and the formation of nuclei that enhances further polymerization, lowering of the pH thus creating a more unstable system and enhancing the diffusion of OH<sup>-</sup> ions.

**Compressive Strength and Specific Surface Area.** Compressive strength values measured for various matrixes seem to follow a very specific trend whereby the compressive strength of a matrix containing K is usually higher than for the same geopolymer mix containing only Na. This trend is obvious from Table 11 if matrixes G1 and F1 are compared and also from Table 12, comparing S4 and S5, S6 and S7, and S8 and S9, as well as S11 and S12. This is not the case as far as a comparison between H1 and H4 as well as H2 and H3 are concerned where this trend seems to be reversed. The fairly high dosage of metal contaminants as well as a different M<sub>2</sub>O/SiO<sub>2</sub> ratio is probably responsible for

**Table 12. Compressive Strengths (MPa) and Specific Surface Area (m<sup>2</sup>/g) after 14 Days as Measured for Selected Matrixes**

matrix	K <sub>2</sub> O/ SiO <sub>2</sub> (mol)	Na <sub>2</sub> O/ SiO <sub>2</sub> (mol)	(K <sub>2</sub> O + Na <sub>2</sub> O)/ SiO <sub>2</sub> (mol)	specific surface area	compressive strength
S4	0.42	0.16	0.58	0.31	4.0
S5	0.00	0.58	0.58	0.16	2.2
S6	1.04	0.16	1.20	1.00	11.0
S7	0.00	1.04	1.04	0.61	8.1
S8	0.89	0.16	1.05	0.68	11.4
S9	0.00	1.04	1.04	0.16	10.6
S11	0.89	0.16	1.05	0.80	11.0
S12	0.00	1.01	1.01	0.34	8.5
S23	1.78	0.16	1.94	0.28	2.0
S36	1.61	0.00	1.61	0.61	36.7
S37	0.60	1.21	1.81	0.12	17.3

**Figure 1.** Relationship between the compressive strength and the ratio K<sub>2</sub>O/SiO<sub>2</sub> at different water contents.

these values and this was discussed in a separate paper.<sup>23</sup> Matrixes S23 and S36 (Table 12) have similar K<sub>2</sub>O/SiO<sub>2</sub> ratios although their compressive strengths differ by a factor of almost 20. Sodium silicate solution was used for matrix S23, and potassium silicate, for matrix S36. Matrix S37 was synthesized using K silicate and an amount of NaOH to give more or less similar M<sub>2</sub>O/SiO<sub>2</sub> ratios for all three matrixes. It is doubtful, however, that the presence of Na (in matrix S23) alone would be responsible for the large difference in compressive strength, and it is concluded therefore that the type of silicate does have an effect on the structure formation. Weldes and Lange<sup>24</sup> noted that there exist substantial differences between the structures of sodium and potassium soluble silicates. Potassium is usually held more firmly in glassy structures, and for similar lower M<sub>2</sub>O/SiO<sub>2</sub> ratios average molecular weights in the metal silicate solution are usually higher for potassium than for sodium silicates, indicating the presence of relatively more polysilicate species. This also agrees with an earlier statement that one would expect a higher degree of condensation in aluminosilicate structures prepared with potassium than those containing mainly sodium. The fact that matrix S37 is substantially stronger than matrix S23 testifies to the fact that the silicate does retain part of its original structure, the latter again being influenced by the type of alkali metal cation present.

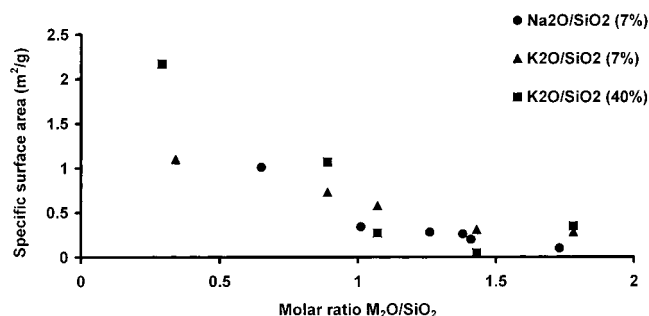
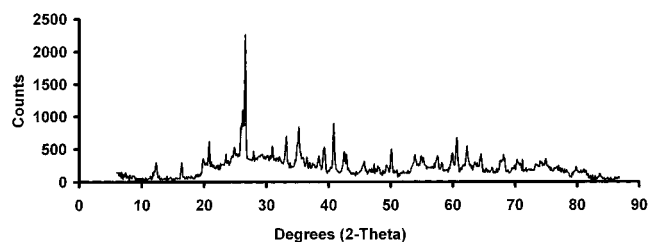
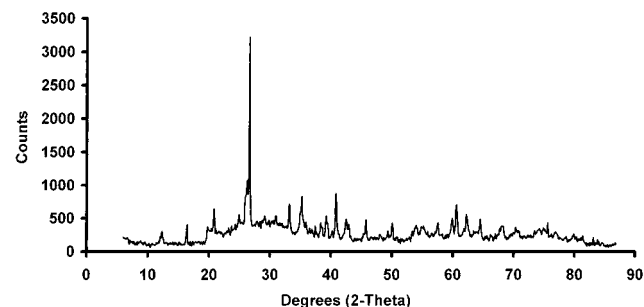
The results presented in Figure 1 were found for both Na- as well as K-containing matrixes, and although different water contents were used, it seems that there exists an optimum M<sub>2</sub>O/SiO<sub>2</sub> ratio for maximum compressive strength. This effect was observed as early as 1940 by Purdon<sup>25</sup> and again points to a certain stoichiometric ratio<sup>3,9</sup> for optimum addition of the alkali metal. When this ratio is exceeded, the excess alkali serves to weaken the structure causing a negative impact on most

**Table 13. Compressive Strengths (MPa) and Specific Surface Area (m<sup>2</sup>/g) after 14 Days as Measured for Selected Matrixes**

matrix	K <sub>2</sub> O/ SiO <sub>2</sub> (mol)	Na <sub>2</sub> O/ SiO <sub>2</sub> (mol)	(K <sub>2</sub> O + Na <sub>2</sub> O)/ SiO <sub>2</sub> (mol)	specific surface area	compressive strength
S31	0.16	1.30	1.46	0.16	1.4
S32	0.32	1.08	1.40	0.23	3.3
S29	0.49	0.84	1.33	0.07	2.1
S33	0.71	0.66	1.37	0.19	10.1
S34	0.89	0.41	1.30	0.87	10.2

physical properties. This optimum ratio of M<sub>2</sub>O/SiO<sub>2</sub> for maximum compressive strength was also observed by Rahier et al.<sup>3</sup> and associated with maximum reaction enthalpy of the exothermic synthesis reaction. The relative influence of K compared to Na can be seen from Table 13, where the K<sub>2</sub>O/SiO<sub>2</sub> ratio is increased and the Na<sub>2</sub>O/SiO<sub>2</sub> ratio decreased, resulting in an almost stepwise increase in strength once a critical concentration of K is reached. This again testifies to the earlier remark that for the matrixes under discussion the K-containing structures seem to be significantly stronger than those containing Na and for such a sudden and large difference one could expect a totally different structure in terms of both chemical and physical properties. Davidovits<sup>9</sup> reported varying thermal properties for geopolymers containing Na and K, the latter having a higher degree of thermal stability resulting in higher fusion temperatures if all other compositional factors remain constant. The fly ash from Tarong, used in the synthesis of matrixes S4–S37 (Tables 4 and 5), also exhibited favorable setting properties (Table 6) in the presence of K, as was discussed earlier, indicating that a more stable structure is formed. These facts, together with the results obtained from compressive strength tests, as discussed above, indicate that matrixes containing K might have a totally different structure than those containing only Na. Computer-generated molecular simulations of various proposed geopolymer structures, published by Davidovits,<sup>9</sup> do indeed support this statement, and further proof of this will be discussed below.

For all comparable matrixes in Tables 11 and 12 the presence of K resulted in a higher specific surface area being measured, something that is unexpected considering that these matrixes were also measured as having higher compressive strengths. In a comparison of matrixes S23, S36, and S37 (Table 12), the presence of Na in matrixes S37 and S23 can be seen to significantly lower the specific surface area and the compressive strength. An increase in the K<sub>2</sub>O/SiO<sub>2</sub> ratio in the matrixes of Table 13 also increases the specific surface area as well as the measured compressive strengths. As one would not expect a structure with a higher internal surface area to be stronger than an identical structure with a lower surface area, the only conclusion is that these two families of structures differ substantially in both a chemical and physical manner. It is interesting to note from Figure 2 that specific surface area seems to decrease with increasing M<sub>2</sub>O/SiO<sub>2</sub> ratio for all matrixes. It also seems that there exists a value of the M<sub>2</sub>O/SiO<sub>2</sub> ratio where the decrease in specific surface area reaches a minimum asymptotic value with further increases in the M<sub>2</sub>O/SiO<sub>2</sub> ratio being less pronounced in terms of changing the specific surface area values of the corresponding matrixes. For similar compositional ratios Figure 2 also suggests that the surface area values of the K-containing matrixes are slightly higher

**Figure 2.** Relationship between the specific surface area and the ratio M<sub>2</sub>O/SiO<sub>2</sub> of matrixes S4–S37 at 7% and 40% clay content.**Figure 3.** X-ray diffraction spectrum of matrix F1.**Figure 4.** X-ray diffraction spectrum of matrix G1.

than those of their Na-containing counterparts. This correlation between higher surface area values for matrixes that have faster setting properties, such as is the case with the K-containing matrixes discussed here, was also suggested by Davidovits although he mentioned mainly Na-containing geopolymers.<sup>26</sup> Mostowicz and Berak<sup>27</sup> observed that for zeolites synthesized with hydroxides of Li, Na, and K the resultant particle size increased in the order Li < Na < K, which could result in a less dense packing and higher specific surface area values for matrixes synthesized with KOH.

**X-ray Diffraction (XRD) and Electron Microscopy.** Due to their amorphous and semiamorphous nature many geopolymers are not suitable for detailed study by X-ray diffraction<sup>3,8,9</sup> although some conclusions can be drawn. A comparison of Figure 3 (matrix F1) and Figure 4 (matrix G1) is representative of what was found for most matrixes in that no new crystalline phases are observed that distinguish either of the matrixes. Peaks present in the starting materials, as is shown in Figure 5, can account for all of the crystalline peaks found in Figures 3 and 4. As was stated earlier,<sup>14</sup> it is expected that fly ash particles are only partially dissolved and therefore a degree of crystallinity is retained in the final product. No crystalline calcium silicate hydrate (CSH) phases were detected, and one has to draw the conclusion that any new phases that formed were largely amorphous to X-rays. When Figure 5 is compared with Figures 3 and 4, the increase in amorphous content between 20 and 40° in 2θ can be



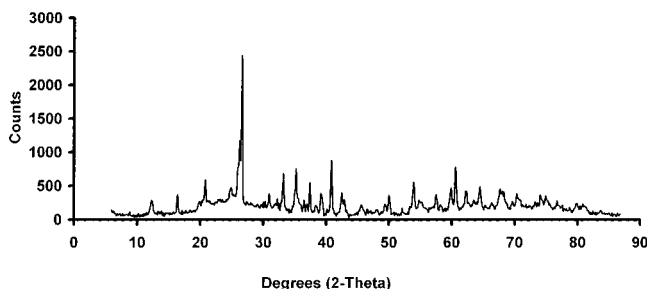


**Figure 5.** Combined X-ray diffraction spectra of kaolinite and fly ash used in matrixes F and G.

seen in the spectra of matrixes G1 and F1. The maximum value of the amorphous "hump" also seems to shift from around  $27.3^\circ$  in  $2\theta$  in Figure 5 to around  $29.3^\circ$  in  $2\theta$  in Figures 3 and 4. This shift is identical for both matrixes, and the value agrees with data published by Davidovits<sup>9</sup> for geopolymers containing K and Na. Rahier et al.<sup>3</sup> mentioned that this value seems to be related to the  $M_2O/SiO_2$  ratio and provided values of around  $29.5^\circ$  in  $2\theta$  for structures with a  $Na_2O/SiO_2 = 1.25$ , which is fairly close to the value of  $29.3^\circ$  in  $2\theta$  obtained for matrixes F1 and G1 where  $M_2O/SiO_2 = 1.14$ . Work published by Davidovits<sup>26</sup> shows no clear relation between the type of alkali metal cation and the maximum value of the amorphous region. This lack of information regarding the various amorphous phases and their chemical compositions was addressed by subjecting samples to electron diffraction studies where chemical analyses of the various phases could be performed.

Matrixes F1 and G1 were examined by electron diffraction and the main phases identified and analyzed for their elemental composition. The results for matrix F1 are presented in Table 14, and those for matrix G1, in Table 15. It is significant to note that most phases contain Na and K, as well as Ca, suggesting that they could be CSH phases similar to those discussed by Richardson et al.<sup>28</sup> for alkali-activated slag pastes. The fly ash used contains around 8% Ca as CaO, and this is much less than the amount usually found in slags. In a comparison of the  $d$  spacings with values published for CSH phases by Richardson et al.<sup>28</sup> and Wang and Scrivener,<sup>16</sup> it is obvious that there are very few similarities between these phases and the ones presented here, presumably because of the lower Ca and higher Na and K content. These results also prove that an amount of Ca is dissolved during synthesis, and it is interesting to note that the Ca is always associated with K while Na is not present in all phases containing Ca. Structural models presented by Davidovits<sup>9</sup> also imply this association between Ca and K. The presence of the added heavy metal is thought to affect the structure<sup>23</sup> and thus the  $d$  spacing values but falls outside the scope of the present discussion. In comparison of the  $d$  spacings for the different phases found in matrix G1 and F1, there seem to be some similarities although none of the phases is structurally identical to another, supporting the earlier statement that the presence and relative amounts of Na and K significantly alter the structural and mechanical properties. Qualitative examination revealed more polycrystalline phases to be present in matrix F1 compared to matrix G1, suggesting that the polycondensation reaction proceeds differently depending on the alkali metal cation present. This is in agreement with an earlier observation by

Rahier et al.<sup>3</sup> that, for the metakaolinite system they studied, the presence of Na resulted in a more complex crystallization process. This could also be the reason for the abundance of phases found in matrix F1. Previous work<sup>3</sup> in this field also suggested that there is some relation between short range order in the final structure and the speed with which the polycondensation reaction occurs, a fact that is also supported by our results. The presence of K in the phases of matrix F1 is thought to originate from the fly ash (Table 1). Although it is obvious from the results presented in Tables 14 and 15 that the relative quantity of Na or K in the synthesis mixture affects the formation of different phases, the exact mechanism by which this occurs is not very well understood. The structure-directing roles played by K and Na ions are complex, as they only seem to affect the short-range order of the structure with the overall structure being largely amorphous or semiamorphous. This role has been acknowledged by Davidovits<sup>10,11</sup> although the exact nature of it is not fully understood.

**Infrared (IR).** The main peaks of consideration during infrared studies of the various matrixes are those associated with bending and stretching modes of the main T–O bonds (where T is either Si or Al) that form the backbone of all aluminosilicate structures. These results are summarized in Table 16 for a range of matrixes. The peaks around  $460\text{--}470\text{ cm}^{-1}$  have been assigned previously<sup>3,29</sup> to the in-plane bending mode of T–O bonds, while the peaks between  $950$  and  $1050\text{ cm}^{-1}$  are attributed<sup>29,30</sup> to asymmetric stretching of T–O bonds. Vibrations in both these regions are considered to originate from within the Si and Al tetrahedra that are the main building blocks of aluminosilicate structures. The region  $1050\text{--}1200\text{ cm}^{-1}$  contains vibrations that have been assigned<sup>29</sup> to asymmetric stretching of linkages between tetrahedra and would thus be influenced by changes in the structural framework. The peak at  $913\text{ cm}^{-1}$  has been assigned<sup>31</sup> to OH-bending bands where the OH groups are bonded to Al.

The bands associated with vibrations originating from within the Al- and Si tetrahedra, such as those at  $460$ ,  $1010$ , and  $1033\text{ cm}^{-1}$  are indicative of the degree of polymerization that has taken place<sup>32</sup> with a higher degree of polymerization associated with a higher energy. This seems to be the case when the peaks found in matrixes F1 and G1, as well as F2 and G2 (Table 16), are compared. Values obtained are fairly similar although there seems to be a slight shift to higher energies in the case of the K-containing matrix G1 (higher T–O-bending frequency than F1) and G2 (higher T–O-stretching frequencies than F2). This trend is also found when comparing matrixes S13–S17 with S18–S23, the latter group displaying peaks in the  $1010$  and  $1033\text{ cm}^{-1}$  range with slightly higher energy. The peaks at  $460\text{ cm}^{-1}$  are less sensitive and do not display this relation very clearly. For these matrixes the higher frequencies of the  $1013$  and  $1087$  peaks, especially at higher K contents, could signify an increased degree of polycondensation due to the presence of K. This also supports the compressive strength results as well as the earlier discussion regarding the higher degree of condensation thought to be caused by K because of its size and coordination with water molecules. These effects are displayed in the results presented for matrixes S36 and S37, where K silicate was used and very little sodium is present in the matrixes. The peaks at  $1012$  and  $1038\text{ cm}^{-1}$  display the highest energies when



**Table 14. Qualitative Electron Diffraction Results for F1**

structure	<i>d</i> -spacings (Å)	composition
amorphous	3.53/2.15/1.23/1.05/0.78/0.69	Al, Si, Cu
polycrystalline	1.27	Al, Si, Na, K, Ca, Mn, Fe, Cu
polycrystalline	4.43/3.90/2.64/1.71/1.57/1.49/1.27/1.20/0.83	Al, Si, Na, K, Ca, Mn, Cu
amorphous	not available	Al, Si, K, Ca, Ti, Fe, Cu
crystalline	not available	Al, Si, Na, K, Ca, Fe

**Table 15. Qualitative Electron Diffraction Results for G1**

structure	<i>d</i> -spacings (Å)	composition
amorphous	4.95/3.86/2.91/2.58/1.66/1.37/1.01	Al, Si, K, Ca, Cu
amorphous to microcrystalline	4.81/3.90/3.42/2.78/2.69/1.82/1.66/1.37/1.27/1.08/0.98/ 0.80/ 0.72/0.64/0.60	Al, Si, K, Ca, Cu
amorphous	4.85/4.02/2.91/2.47/1.87/1.66/1.35/1.15/0.97/0.81/0.70	Al, Si, Na, K, Ca, Fe, Ti

**Table 16. FTIR Results for Selected Matrixes (cm<sup>-1</sup>)**

matrix	K <sub>2</sub> O/SiO <sub>2</sub> (mol)	Na <sub>2</sub> O/SiO <sub>2</sub> (mol)	(K <sub>2</sub> O + Na <sub>2</sub> O)/SiO <sub>2</sub> (mol)	T–O bending	OH bending	T–O stretching		
F1	0.00	1.14	1.14	466	914	1010	1031	
G1	0.97	0.17	1.14	472	913	1010	1031	
F2	0.00	1.14	1.14	470	914	1010	1031	
G2	0.97	0.17	1.14	470	913	1012	1033	
S13	0.00	0.65	0.65	467	915	1009	1035	1087
S15	0.00	1.26	1.26	466	914	1009	1034	1088
S14	0.00	1.38	1.38	467	912	1009	1035	1087
S16	0.00	1.41	1.41	466	912	1011	1032	1083
S17	0.00	1.73	1.73	467	912	1011	1032	1080
S18	0.34	0.18	0.52	469	913	1010	1037	1091
S19	0.89	0.16	1.05	467	913	1010	1035	1091
S21	1.07	0.15	1.22	466	913	1009	1035	1085
S22	1.43	0.16	1.59	467	913	1011	1035	1090
S23	1.78	0.16	1.94	464	913	1013	1030	1087
S31	0.16	1.30	1.46	469	913	1009		1092
S32	0.32	1.08	1.40	470	913	1009		1091
S29	0.49	0.84	1.33	471	913	1009		1093
S33	0.71	0.66	1.37	469	913	1009		1093
S34	0.89	0.41	1.30	471	913	1009		1096
S36	1.61	0.00	1.61	466	915	1012	1038	1088
S37	0.60	1.21	1.81	467	913	1012	1037	1085

compared to any of the other matrixes. This indicates that for this specific fly ash the presence of K definitely increases the extent or degree of polymerization and also supports an earlier statement that some of the structure of the original silicate used is thought to be retained in the final product. Matrixes S29–34 do not display this relation for different ratios of K<sub>2</sub>O/Na<sub>2</sub>O while the total M<sub>2</sub>O/SiO<sub>2</sub> ratio remains largely constant. It is also interesting to note that the peaks at 1033 cm<sup>-1</sup> for matrixes S13–17 and S18–23 seem to gradually shift to lower energies as the M<sub>2</sub>O/SiO<sub>2</sub> ratio is increased. The reason for this is an increasing number of tetrahedral Al substituting for Si as both the alkalinity and number of charge balancing ions increase.

The portion of the spectra at 1090 cm<sup>-1</sup> are sensitive to vibrations of linkages between tetrahedra as well as the topology and mode of arrangement of the secondary building blocks of the structure. For matrixes S13–17 and S18–23 there seems to be a slight decrease as the M<sub>2</sub>O/SiO<sub>2</sub> ratio is increased, with the values for K-containing matrixes again being slightly higher than that for matrixes containing mainly Na. This is an indication that there do exist some structural differences that require more energy for the stretching of bonds between structural units in K-containing matrixes. Again this explains the higher compressive strengths measured for K-containing matrixes and also suggests that some structural differences exist with relation to the specific surface area measurements. The exact nature of these structural differences, in terms of secondary building units, is still unknown although an increase in the K/Na ratio in matrixes S29–34 also

shows an increase in the energy requirement of this absorption band. This again suggests that the presence of K does serve to strengthen the bonds between this secondary building units, a fact that is portrayed in the compressive strength results.

The band at 913 cm<sup>-1</sup> does not seem to be affected by changes in the M<sub>2</sub>O/SiO<sub>2</sub> ratio except for matrixes with no K present, such as matrixes S13–17, and matrixes without any Na present, such as S36. The frequency of this band originates from the bending of Al–OH bonds, while the manner in which the presence of pure solutions of Na and K affects the substitution and immediate environment of bound Al in order to cause changes in the frequency of this vibration is unknown.

#### Environmental Leaching and Acid Resistance.

To determine the effect of the type of alkali metal cation on the ability of geopolymers to immobilize heavy metals two sets of tests were conducted as was described above. Table 17 summarizes the effect of a changing M<sub>2</sub>O/SiO<sub>2</sub> ratio on the acid resistance of matrixes containing Na and K cations when tested by submerging in HCl. The fly ash used in this synthesis was discussed earlier as exhibiting a faster setting reaction with NaOH as opposed to KOH, indicating that a more stable final structure might be produced. This was indeed the case with the Na-containing matrixes B26–31 having a higher acid resistance when compared to B32–37, containing K. With reference to Table 17, there seems to be an optimum M<sub>2</sub>O/SiO<sub>2</sub> ratio for which the acid resistance of a matrix will be a maximum. Values less than this would create an incomplete, weaker structure through lack of enough OH ions to dissolve the neces-

**Table 17. Results of Acid Resistance Testing for Matrixes Manufactured from Macquarie Fly Ash as % Mass Loss after Immersion in 1 M HCl for 34 Days**

matrix	alkali hydroxide	(K <sub>2</sub> O + Na <sub>2</sub> O)/SiO <sub>2</sub> (mol)	% mass loss
B26	Na	0.23	1.0
B27	Na	0.30	0.4
B28	Na	0.36	0.1*
B29	Na	0.43	0.4
B30	Na	0.50	0.4
B31	Na	0.57	0.8
B32	K	0.21	3.7
B33	K	0.26	4.9
B34	K	0.31	1.1
B35	K	0.35	0.2*
B36	K	0.40	1.5
B37	K	0.45	2.7

**Table 18. Equilibrium Concentrations Achieved during Leaching with Acetic Acid for 24 h (ppm)**

matrix	contaminant	212/600 $\mu\text{m}$	1700/2360 $\mu\text{m}$
F1	Cu	17	11
F2	Pb	11	8
G1	Cu	12	9
G2	Pb	<7	<7

**Table 19. Equilibrium Concentrations Achieved during Leaching with Hydrochloric Acid for 24 h (ppm)**

matrix	contaminant	600/1000 $\mu\text{m}$	2360/2800 $\mu\text{m}$
F1	Cu	22	27
F2	Pb	14	6
G1	Cu	32	17
G2	Pb	26	10

sary precursors as well as a lack of Na or K ions to allow for substitution of Si by Al. A ratio larger than the optimum would again provide pockets of excess alkali in the structure that are very susceptible to attack by acids, reducing the measured acid resistance, apart from the fact that this optimum M<sub>2</sub>O/SiO<sub>2</sub> ratio can be seen to exist for both K- and Na-containing matrixes, with both sets of matrixes exhibiting the same value of M<sub>2</sub>O/SiO<sub>2</sub> = 0.35. This again points to some kind of preferred stoichiometric combination of reagents. It has been reported<sup>24</sup> that K-containing silicates usually exhibit better acid resistance when sulfuric acid or carbon dioxide is considered because of the tendency of Na to form hydrated salts with these acids, a property K does not have.

The previous statement becomes apparent when Table 18 is considered and acetic acid leach results for matrixes F1 and G1 as well as F2 and G2 are compared. In each case the heavy metal is better immobilized in the matrixes containing K, i.e., G1 and G2. When the same matrixes are submitted to testing by HCl (Table 19), however, an exact reversal of the results is obtained with the Na-containing matrixes F1 and F2 generally exhibiting the better immobilization efficiencies. This indicates that choosing the type of alkali metal cation could play an important role in the future stability of geopolymeric immobilization systems depending on the perceived conditions that the structure will encounter. The long-term stability will also depend in part on the type of fly ash and starting materials being used as well as the type of heavy metal being immobilized. This aspect was briefly discussed in an earlier publication<sup>14</sup> which concluded that the complicated relationship between the metal being immobilized and other variables that affect the structure and leaching properties,

such as the type of alkali cation, is still not fully understood.

## Conclusions

It is evident that the type of alkali metal cation affects every stage of the geopolymerization of fly ash. During dissolution fly ashes from different sources will dissolve with different ratios of Al/Si, depending on the type of alkali metal present, and this is again thought to have an effect on the speed with which the condensation reaction will occur. During synthesis the alkali metal cations are thought to play a very important role in first ordering water molecules and later soluble silicate species to start the nucleation process that will lead to structure formation. During this stage the cation is playing a very important role in determining the final structure and serves as a template in both a directing and controlling capacity as far as polycondensation and crystal growth is concerned. The size of the cation also affects the eventual crystal morphology with K seemingly responsible for a higher degree of condensation when compared to Na under the same conditions. Matrixes containing K had higher compressive strengths but also higher specific surface area values and proved to have a lower degree of crystallinity as well as a lower resistance to attack by HCl. The choice of type of alkali metal cation to be used during synthesis will depend on many factors, the most important being the type of source materials to be used as well as the final objective in terms of application. Apart from allowance of the substitution of Al for Si to take place in aluminosilicate structures, the single most important role played by alkali metal cations is their structure-directing effect during synthesis as this eventually affects most chemical and physical properties of the final product.

## Literature Cited

- (1) Barrer, R. M. *Hydrothermal Chemistry of Zeolites*; Academic Press: London, 1982.
- (2) Breck, D. W. *Zeolite Molecular Sieves*; John Wiley and Sons: London, 1974.
- (3) Rahier, H.; Simons, B.; Biesemans, M.; Van Mele, B. Low-Temperature Synthesised Aluminosilicate Glasses: Part III Influence of the Composition of the Silicate Solution on Production, Structure and Properties. *J. Mater. Sci.* **1997**, *32*, 2237.
- (4) McCormick, A. V.; Bell, T. The Solution Chemistry of Zeolite Precursors. *Catal. Rev. Sci. Eng.* **1989**, *31*, 97.
- (5) Barrer, R. M. Synthesis of Zeolites. In *Zeolites*; Drzaj, B. et al., Eds.; Elsevier Science Publishers: New York, 1985, p 12.
- (6) Hu, H. C.; Lee, T. Y.; Synthesis Kinetics of Zeolite A. *Ind. Eng. Chem. Res.* **1990**, *29*, 749.
- (7) Van Jaarsveld, J. G. S.; Van Deventer, J. S. J.; Lorenzen, L. The Potential Use of Geopolymeric Materials to Immobilise Toxic Metals: Part I. Theory and Applications. *Miner. Eng.* **1997**, *10*, 659.
- (8) Van Jaarsveld, J. G. S.; Van Deventer, J. S. J.; Lorenzen, L. Factors Affecting the Immobilisation of Metals in Geopolymerised Fly Ash. *Met. Mater. Trans. B* **1998**, *29*, 283.
- (9) Davidovits, J. Geopolymers: Inorganic Polymeric New Materials. *J. Thermal Anal.* **1991**, *37*, 1633.
- (10) Davidovits, J. Mineral Polymers and Methods of Making Them. U.S. Patent 4349386, 1982.
- (11) Davidovits, J. Synthetic Mineral Polymer Compound of the Silicoaluminates Family and Preparation Process. U.S. Patent 4472199, 1984.
- (12) CANMET; Canada, DSS Contract No. 23440-6-9195/01SQ, Preliminary Examination of the Potential Use of Geopolymers for Use in Mine Tailings Management. Final Report, 1988.
- (13) Khalil, M. Y.; Merz, E.; Immobilization of Intermediate-Level Wastes in Geopolymers. *J. Nucl. Mater.* **1994**, *211*, 141.

- (14) Van Jaarsveld, J. G. S.; Van Deventer, J. S. J. The Potential Use of Geopolymeric Materials to Immobilise Toxic Metals: Part II. Material and Leaching Characteristics. *Miner. Eng.* **1999**, *1*, 75.
- (15) Antonic, T.; Cizmek, A.; Subotic, B. Dissolution of Amorphous Zeolite Precursors in Alkaline Solutions: Part II Mechanism of the Dissolution. *J. Chem. Soc., Faraday Trans.* **1994**, *90*, 1973.
- (16) Wang, S.-D.; Scrivener, K. L.; Hydration Products of Alkali-Activated Slag. *Cem. Concr. Res.* **1995**, *25*, 561.
- (17) Kostinko, J. A.; Factors Influencing the Synthesis of Zeolites A, X and Y. In *Intrazeolite Chemistry*; Stucky, G. D., et al., Eds.; ACS Symposium Series 218, American Chemical Society: Washington, DC, 1983.
- (18) De Kretser, R. The Rheological Properties and De-watering of Slurried Coal Wire Tailings. Ph.D. Thesis, The University of Melbourne, Victoria, Australia, 1995.
- (19) Australian Standard AS 1012.9; Methods for testing concrete, 1986.
- (20) Appendix 1 to Part 268, U.S. Federal Register, Nov 7, 1986, Vol. 51, p 216.
- (21) Ramachandran, V. S. Accelerators. In *Concrete Admixtures Handbook*; Ramachandran, V. S., Ed., Noyes Publications: Westwood, NJ, 1984.
- (22) Popovics, S. Concrete Making Materials; McGraw-Hill: Sydney, 1979.
- (23) Van Jaarsveld, J. G. S.; Van Deventer, J. S. J. The Effect of Metal Contaminants on the Formation and Properties of Waste Based Geopolymers. *Cem. Concr. Res.* 1999, in press.
- (24) Weldes, H. H.; Lange, K. R.; Properties of Soluble Silicates. *Ind. Eng. Chem.* **1969**, *61*, 29.
- (25) Purdon, A. O. The Action of Alkalis on Blast-Furnace Slag. *J. Soc. Chem. Ind.* **1940**, *59*, 191.
- (26) Davidovits, J. Structural Characterisation of Geopolymeric Materials with X-ray Diffractometry and MAS NMR Spectroscopy. *Geopolymer '88: First European Conference on Soft Mineralurgy*; Universite de Technologie De Compiègne: Compiègne, France, 1988, Vol. 2, 149.
- (27) Mostowicz, R.; Berak, J. M. Factors Influencing the Crystal Morphology of ZSM-5 Type Zeolites. In *Zeolites*; Drzaj, B., et al., Eds.; Elsevier Science Publishers: New York, 1985; p 65.
- (28) Richardson, I. G.; Brough, A. R.; Groves, G. W.; Dobson, C. M. The Characterisation of Hardened Alkali-activated Blast-furnace Slag Pastes and the Nature of the Calcium Silicate Hydrate (CSH) Phase. *Cem. Concr. Res.* **1994**, *24*, 813.
- (29) Flanigan, E. M.; Khatami, H.; Szymanski, H. A. *Molecular Sieve Zeolites*, Advances in Chemistry Series; American Chemical Society: Washington, DC, 1971; Vol. 101, p 201.
- (30) Palomo, A.; Macias, A.; Blanco, M. T.; Puertas, F.; Physical, Chemical and Mechanical Characterisation of Geopolymers. *Proc. 9th Int. Congr. Chem. Cem.* **1992**, 505.
- (31) Madani, A.; Aznar, A.; Sanz, J.; Serratos, J. M.  $^{29}\text{Si}$  and  $^{27}\text{Al}$  NMR Study of Zeolite Formation from Alkali-leached Kaolinites. Influence of Thermal Preactivation. *J. Phys. Chem.* **1990**, *94*, 760.
- (32) Ortego, J. D.; Barroeta, Y.; Leaching Effects on Silicate Polymerisation. An FTIR and  $^{29}\text{Si}$  NMR Study of Lead and Zinc in Portland Cement. *Environ. Sci. Technol.* **1991**, *25*, 1171.

Resubmitted for review June 21, 1999

Accepted June 21, 1999

IE980804B